Intercomparison of ILAS-II version 1.4 aerosol extinction coefficient at 780 nm with SAGE II, SAGE III, and POAM III

N. Saitoh,[1,2] S. Hayashida,[3] T. Sugita,[1] H. Nakajima,[1] T. Yokota,[1] M. Hayashi,[4] K. Shiraishi,[4] H. Kanzawa,[5] M. K. Ejiri,[6] H. Irie,[7] T. Tanaka,[1] Y. Terao,[8] R. M. Bevilacqua,[9] C. E. Randall,[10] L. W. Thomason,[11] G. Taha,[12] H. Kobayashi,[13] and Y. Sasano[1]

Received 2 June 2005; revised 25 January 2006; accepted 15 February 2006; published 7 June 2006.

[1] The Improved Limb Atmospheric Spectrometer (ILAS)-II on board the Advanced Earth Observing Satellite (ADEOS)-II observed stratospheric aerosol in visible/near-infrared/infrared spectra over high latitudes in the Northern and Southern hemispheres, intermittently from January to March and continuously from April through October 2003. This study assesses the data quality of ILAS-II version 1.4 (V1.4) aerosol extinction coefficient at 780 nm. In the Northern Hemisphere (NH), aerosol extinction coefficient (AEC) from ILAS-II agreed with extinctions from SAGE II and SAGE III within ±10% and with extinction from POAM III within ±15% at heights below 20 km. From 20 to 26 km, ILAS-II AEC was smaller than extinctions from the other three sensors; differences between ILAS-II and SAGE II ranged from 10% at 20 km to 34% at 26 km in the NH. Over the Southern Hemisphere (SH), ILAS-II AEC from 20 to 25 km in February was 12–66% below SAGE II extinction. The difference increased with increasing altitude. Comparisons between ILAS-II and POAM III from January to May in the SH ("non-PSC season") yielded qualitatively similar results. From June to October ("PSC season"), ILAS-II extinction was also smaller than POAM III extinction above 17 km; however, ILAS-II extinction agreed with POAM III extinction to within ±15% from 12 to 17 km during the PSC season. The comparisons indicate that in both hemispheres the ILAS-II V1.4 AEC is comparable to extinctions from other measurements below approximately 20 km and systematically low above approximately 20 km although the mean difference is as small as $\sim 2 \times 10^{-5}$ km^{-1} during the non-PSC season.

Citation: Saitoh, N., et al. (2006), Intercomparison of ILAS-II version 1.4 aerosol extinction coefficient at 780 nm with SAGE II, SAGE III, and POAM III, *J. Geophys. Res.*, *111*, D11S05, doi:10.1029/2005JD006315.

1. Introduction

[2] Stratospheric aerosols greatly impact stratospheric chemistry, including destruction of ozone. In polar regions, Polar Stratospheric Clouds (PSCs), which form under cold conditions in winter and early spring, lead to severe ozone depletion by providing the surface required for heterogeneous reactions that convert inactive chlorine into active chlorine [e.g., *Solomon*, 1999]. Moreover, PSCs irreversibly remove nitric acid from the gas phase through sedimentation (denitrification) [*Solomon*, 1999], and the removal could facilitate springtime ozone depletion [*World Meteorological Organization*, 2002]. Observation of stratospheric aerosols, particularly PSCs, is thus crucial for the understanding of ozone destruction processes. Many stratospheric aerosol measurements have been performed with lidar and Optical Particle Counter (OPC) [*Stratospheric Processes and their Role in Climate*, 2005, and references therein]. Space-borne sensors that provide observations over a large area have also monitored stratospheric aerosols. The Stratospheric Aerosol Measurement (SAM) II is a solar occultation sensor on board a polar-orbiting satellite. It continuously observed stratospheric aerosols and PSCs over

[1]National Institute for Environmental Studies, Tsukuba, Japan.
[2]Now at Center for Climate System Research, University of Tokyo, Kashiwa, Japan.
[3]Faculty of Science, Nara Women's University, Nara, Japan.
[4]Faculty of Science, Fukuoka University, Fukuoka, Japan.
[5]Department of Earth and Environmental Science, Graduate School of Environmental Studies, Nagoya University, Nagoya, Japan.
[6]Center for Atmospheric and Space Sciences, Utah State University, Logan, Utah, USA.
[7]Frontier Research Center for Global Change, Japan Agency for Marine-Earth Science and Technology, Yokohama, Japan.
[8]Division of Engineering and Applied Science and Technology, Harvard University, Cambridge, Massachusetts, USA.
[9]Naval Research Laboratory, Washington, D. C., USA.
[10]Laboratory for Atmospheric and Space Physics, University of Colorado, Boulder, Colorado, USA.
[11]NASA Langley Research Center, Hampton, Virginia, USA.
[12]Science Systems and Applications, Inc., Lanham, Maryland, USA.
[13]Central Research Institute of Electric Power Industry, Tokyo, Japan.

0148-0227/06/2005JD006315$09.00

high latitudes for about 15 years from October 1978 to December 1993 [e.g., *McCormick et al.*, 1982; *Poole and Pitts*, 1994]. Subsequently, several other solar occultation sensors, including the Polar Ozone and Aerosol Measurement (POAM) II (September 1993 to November 1996) [*Randall et al.*, 1996, 2000; *Fromm et al.*, 1997, 1999], the Improved Limb Atmospheric Spectrometer (ILAS) (November 1996 to June 1997) [*Hayashida et al.*, 2000; *Saitoh et al.*, 2002], and POAM III (April 1998 to present) [*Randall et al.*, 2001; *Bevilacqua et al.*, 2002; *Strawa et al.*, 2002] have obtained stratospheric aerosol and PSC data for latitudes similar to those covered by SAM II. In addition, the Stratospheric Aerosol and Gas Experiment (SAGE) II, a solar occultation sensor on board an inclined-orbiting satellite that can make more extensive observations from low/mid latitudes to high latitudes, began regular observations of stratospheric aerosols in October 1984 [e.g., *Thomason*, 1991; *Hitchman et al.*, 1994; *Thomason et al.*, 1997] and is still in operation. SAGE III, which is the successor to SAGE II on board a polar-orbiting satellite, has measured stratospheric aerosols since February 2002 at high latitudes in the Northern Hemisphere (NH) [*Poole et al.*, 2003] and at mid latitudes in the Southern Hemisphere (SH) [*Thomason and Taha*, 2003].

[3] ILAS-II [*Sasano et al.*, 2001] is the successor to ILAS [*Sasano et al.*, 1995, 1999], and was launched on board the Advanced Earth Observing Satellite (ADEOS)-II (polar-orbiting satellite) on 14 December 2002 [*Nakajima et al.*, 2004]. It made about 150 preoperational observations from January to March, and measured continuously for about 7 months from 2 April through 24 October 2003, at which time ADEOS-II lost its function because of solar paddle failure. ILAS-II is designed to observe profiles of stratospheric minor gases such as O_3, HNO_3, NO_2, N_2O, CH_4, H_2O, CFC-11, CFC-12, $ClONO_2$, and N_2O_5 as well as profiles of extinction by stratospheric aerosols and PSCs at high latitudes of both hemispheres (53.9–71.1°N and 63.6–88.0°S). ILAS-II carried three infrared spectrometers (ch.1: 6.21–11.76 μm, ch.2: 3.00–5.70 μm, ch.3: 12.78–12.85 μm), one visible spectrometer (ch.4: 753–784 nm), and a sun-edge sensor [*Nakajima et al.*, 2006]. Aerosol extinction coefficient (AEC) is retrieved from eight different spectral window element data; one of them is at 780 nm in the visible spectrometer and the others are at 3.0, 3.8, 5.1, 7.1, 8.3, 10.6, and 11.8 μm in the infrared spectrometers. In this study, we assess the data quality of ILAS-II AEC at 780 nm processed with the version 1.4 (V1.4) retrieval algorithm.

[4] In this paper, data quality was assessed over the NH by comparing ILAS-II AEC with SAGE II, SAGE III, and POAM III. Over the SH, ILAS-II data were examined in two separate groups. The first group included data from January through May, when PSCs do not occur (hereafter referred to as the "non-PSC season"). ILAS-II AEC data from the non-PSC season were compared to SAGE II and POAM III extinction data. In addition, an OPC and a Laser Particle Counter (LPC) measured aerosol number density profiles in various diameter ranges over Syowa Station on 22 February 2003. These data were converted into extinction at 780 nm and compared to the nearest ILAS-II AEC data obtained on the same day. The second group included data from June through October, when PSCs are frequently observed ("PSC season"). During the PSC season, it is difficult to complete comparisons with other measurements because of the inhomogeneity of PSCs. Almost all the ILAS-II and POAM III profiles during the PSC season included enhanced layers suggesting the existence of PSCs. However, we made statistical comparisons between ILAS-II and POAM III for these PSC profiles rather than individual comparisons.

2. ILAS-II Aerosol Extinction Data and Characteristics

[5] ILAS-II measures solar radiance in the exosphere (direct sunlight) and radiance attenuated as sunlight travels through the atmosphere as a function of tangent height. Sunlight incident on the entrance slit of the visible spectrometer is dispersed by the spectrometer grating, and then detected with a 1024-element metal-oxide-semiconductor (MOS) photodiode array with spectral resolution of ~0.06 nm. The entrance slit size corresponds to an instantaneous field of view (IFOV) of 1 km in the vertical and 2 km in the horizontal at a tangent point. *Nakajima et al.* [2006] detailed the ILAS-II hardware characteristics and its performance in orbit.

[6] The visible spectrometer of ILAS-II measures temperature and pressure by obtaining the absorption spectrum by oxygen molecules (O_2 A-band). Simultaneously, AEC is retrieved from transmittance averaged for 12 elements at approximately 780 nm, outside the O_2 A-band. The ILAS-II algorithm to retrieve AEC from the spectral data obtained with the visible spectrometer is similar to the algorithm used for ILAS data [*Hayashida et al.*, 2000; *Yokota et al.*, 2002]. ILAS-II can measure solar luminosity of the whole solar disk in the exosphere (solar scan data acquisition) [*Nakajima et al.*, 2006]. Thus sunspot and limb darkening effects on the AEC data can be estimated from the measured solar luminosity in the ILAS-II retrieval, while theoretical luminosity was used in the ILAS retrieval. T. Yokota et al. (Improved Limb Atmospheric Spectrometer-II (ILAS-II) version 1.4 algorithm for retrieval of gas and aerosol profiles in the stratosphere, manuscript in preparation, 2006) discussed the improvements of the ILAS-II AEC retrieval over the ILAS retrieval.

[7] In the ILAS AEC data product, "internal error" was provided, which comprises random noise in the observed solar signals, error in the estimate of direct sunlight during atmospheric transmission (100% level), and error in the estimate of ozone absorption in the Wulf band [*Hayashida et al.*, 2000; *Yokota et al.*, 2002]. In the ILAS-II V1.4 product, "repeatability error" is defined and provided instead of the internal error; it is estimated on the basis of measurement repeatability. In addition, error in the estimate of Rayleigh scattering by atmospheric molecules is estimated from uncertainties in the United Kingdom Meteorological Office (Met Office) temperature data that we assume; assumed uncertainties in temperature of ±2 K at 10 km and ±5 K at 70 km resulted in errors of two orders of magnitude smaller than extinction values below ~20 km [*Yokota et al.*, 2002, Figure 6]. This error is provided as "external error" in the ILAS-II product, as in the case of the ILAS product. The Root-Sum-Square (RSS) of the repeatability and external errors is defined as the "total error" (T. Yokota et al., manuscript in preparation, 2006).

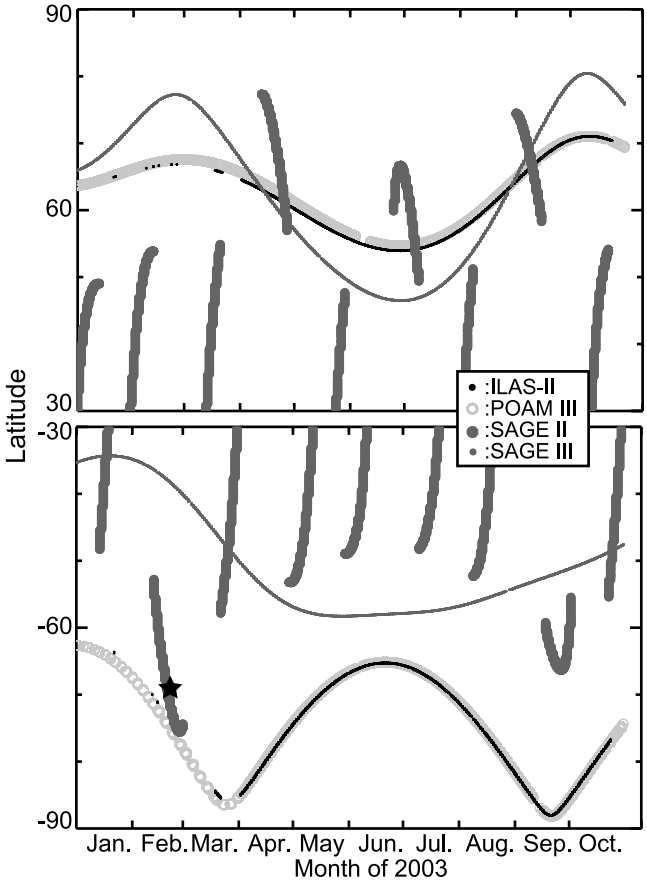

Figure 1. Time series of latitudinal coverage of ILAS-II (black dots), POAM III (light gray circles), SAGE II (thick gray line), and SAGE III (solar occultation mode only; thin gray line) during ILAS-II operations from January to October in 2003. The star denotes the position of Syowa Station (69.0°S, 39.6°E), where the OPC/LPC measurement was conducted on 22 February.

[8] Measurement repeatability is defined as the "closeness of the agreement between the results of successive measurements of the same measurand" [*International Organization for Standardization*, 1993]. Measurement repeatability was calculated empirically in the ILAS-II V1.4 retrieval as follows. The mean (referred to as "$\bar{x}$") and 1σ standard deviation ("σ") of ILAS-II AEC data were calculated for every successive 100 occultation events (~7–8 days) at each altitude level in each hemisphere. The smallest value of relative standard deviation defined as $\varepsilon = \sigma/\bar{x}$ was selected for each altitude level and defined as the measurement repeatability of the altitude level. In this way, the ε value calculated for the period when variability in AEC was smallest during ILAS-II operations is selected as the measurement repeatability. Here, the measurement repeatability is regarded as the precision of the ILAS-II AEC measurements. It includes the contribution from natural variability to some extent and therefore would give an upper limit of the true measurement precision. The precision was 5–15% at 12–26 km in the NH and 6–20% at 12–23 km in the SH (T. Yokota et al., manuscript in preparation, 2006); the precision was smaller than 10% between 15 and 25 km in the NH and between 15 and 21 km in the SH.

[9] At almost all altitudes below 25 km, the magnitude of the measurement repeatability over the SH was larger than the magnitude over the NH (e.g., five times larger at 25 km). ILAS-II made continuous observations for less than an entire year, only for seven months from April to October. The values of the measurement repeatability over the SH were estimated from data obtained in April or in October when the atmosphere is sometimes perturbed because of the formation or break up of the polar vortex at ILAS-II measurement latitudes. In contrast, the values of the measurement repeatability over the NH were estimated from data acquired primarily in the summer (July to October), a more quiescent time of year. The values of the measurement repeatability over the SH reflect larger variability in atmospheric aerosol compared to the NH because of the seasons sampled.

[10] This study focused on AEC data below 30 km in the NH and below 25 km in the SH to avoid the effect of sunspots. At least about one sixth of all the ILAS-II AEC data at 780 nm are affected by sunspots judging from the observed solar luminosity data. Sunspots effect on the AEC data can be estimated from the solar luminosity in the ILAS-II retrievals (T. Yokota et al., manuscript in preparation, 2006), but the effect cannot always be corrected in the current version because of a hardware problem on ILAS-II [*Nakajima et al.*, 2006]. In the current version, most of the AEC data still include sunspots effect above ~30 km in the NH and above ~25 km in the SH. Sunspots could affect ILAS-II AEC data at lower altitude levels in the SH compared to the NH, probably because ILAS-II AEC values in the SH were generally smaller than those in the NH at the same altitude levels. Those disturbed data are not recommended for scientific use.

3. Data for Comparison

[11] Figure 1 shows latitudinal coverage of ILAS-II (black dots), POAM III (light gray circles), SAGE II (thick gray line), and SAGE III (solar occultation measurements only; thin gray line) during ILAS-II operations from January to October 2003. POAM III observations occurred at similar latitudes and times as ILAS-II in both hemispheres. Coincident pairs of ILAS-II and POAM III observations were chosen when the distance between the two measurement locations was less than 150 km and the time difference was less than 1 hour in the NH and the non-PSC season in the SH. A more stringent criterion for coincident pairs was applied during the PSC season in the SH because of the spatial inhomogeneity of PSCs. Here, a maximum distance of 50 km and a maximum time difference of 1 hour were applied for the selection. Comparisons in the NH only used aerosol data after mid-April. The polar vortex, as defined by the definition of *Nash et al.* [1996], persisted at approximately 20 km at ILAS-II measurement latitudes until mid-April. At the boundary of the polar vortex, large gradients in stratospheric aerosol concentration exist [*Thomason and Poole*, 1993].

[12] SAGE II and SAGE III usually made observations at greater distances from ILAS-II measurements than POAM III did owing to the difference in satellites' orbit. Thus the distance constraint between the two measurement locations was set to be 300 km, although the same 1-hour maximum

time difference was used. These criteria yielded sufficient numbers of coincident pairs in the NH. For the SH, however, the criteria yielded only a few coincident pairs. Thus looser criteria were applied. Coincident pairs in the SH were required to be within 500 km of each other, with a time difference of at most 12 hours. These looser criteria allowed multiple SAGE II observations to match a single ILAS-II data point. In that case, all observations were accepted as individual pairs.

[13] SAGE II does not observe aerosol extinction at 780 nm. SAGE II extinction data at 525 nm and 1019 nm were interpolated to extinction at 780 nm by assuming that the logarithm of aerosol extinction is roughly proportional to the logarithm of wavelength in the lower stratosphere, as in the works by *Burton et al.* [1999] and *Hayashida et al.* [2000]. The reported errors of SAGE II extinction data were also interpolated. This study uses SAGE II version 6.2 (V6.2) aerosol extinction data. Although the V6.2 extinction data have not yet been validated, we can confirm the reliability of the data set by comparing to the previous versions of 5.93 [e.g., *Osborn et al.*, 1989; *Ackerman et al.*, 1989; *Russell and McCormick*, 1989] and 6.0 [*Hervig and Deshler*, 2002] extinction data that have no clear bias at the two relevant wavelengths. The V6.2 extinction data agreed to the V5.93 data within the RSS of both reported errors. The difference was within ~10% from 18 to 30 km, although the V6.2 extinction data were on average smaller than the V5.93 data below 18 km. Better agreement was seen in comparisons between the V6.2 and the V6.0 below 18 km, although the V6.2 extinction data were on average larger than the V6.0 data above 25 km. We can conclude that SAGE II V6.2 extinction data interpolated to 780 nm should have no systematic bias.

[14] SAGE III aerosol extinction data and errors at 756 nm and 869 nm were interpolated to extinction at 780 nm using a method similar to that applied to SAGE II extinction data. SAGE III version 3.0 (V3.0) aerosol extinction data are used in this study. These data, nearly identical to the V2.0 data [*Taha et al.*, 2004], have a positive bias at all altitudes at 756 nm and a negative bias above 24 km at 869 nm; extinctions at these two wavelengths do not follow the power law that is determined from extinctions at the other SAGE III wavelengths [*Thomason and Taha*, 2003]. The positive bias in extinction at 756 nm and no bias at 869 nm below 24 km should produce a slightly positive bias in extinction interpolated to 780 nm. Here, bias in SAGE III extinction data interpolated to 780 nm was estimated by comparing the interpolated values to SAGE II extinction data interpolated to 780 nm. April and September SAGE II and SAGE III measurements yielded 32 coincident pairs in the NH when a distance maximum of 300 km and a time difference maximum of 1 hour were applied as criteria for the data from April to October 2003. The relative difference, $D_{SAGE3\text{-}SAGE2}$ (%), is as follows:

$$D_{SAGE3\text{-}SAGE2}(\%) \equiv \frac{100 \times (\text{SAGE III} - \text{SAGE II})}{\text{SAGE II}}.$$

$D_{SAGE3\text{-}SAGE2}$ was calculated for all 32 coincident pairs. Figure 2a shows close agreement between SAGE III and SAGE II extinction data above 12 km during ILAS-II operations, although SAGE III extinction was slightly larger at almost all altitude levels, as expected.

[15] POAM III measures aerosol extinction at 780 nm, so a direct comparison can be made with ILAS-II AEC data. POAM III aerosol extinction data (version 4.0, abbreviated as V4.0) at 780 nm used in this study have not been validated through intercomparisons with other measurements. Here, POAM III extinction data at 780 nm were also compared with SAGE II extinction data interpolated to 780 nm. Comparison criteria in the NH were a distance maximum of 300 km and a time difference maximum of 1 hour, yielding 21 total coincident pairs in April, July, and September 2003. Comparison criteria in the SH were a distance maximum of 500 km and a time difference maximum of 12 hours, which yielded 38 coincident pairs in February. The relative difference between SAGE II and POAM III, $D_{POAM3\text{-}SAGE2}$ (%), was calculated for all coincident pairs as follows:

$$D_{POAM3\text{-}SAGE2}(\%) \equiv \frac{100 \times (\text{POAM III} - \text{SAGE II})}{\text{SAGE II}}.$$

As shown in Figure 2b, POAM III extinction agreed with SAGE II extinction in the NH to within 1σ standard deviation, although POAM III extinction was 14–22% larger on average than SAGE II extinction from 22 to 24 km. In contrast, from 13 to 23 km in the SH, POAM III extinction was more than 1σ standard deviation than SAGE II extinction, as shown in Figure 2c; POAM III extinction data clearly showed a 11–30% systematic positive bias relative to SAGE II extinction data. These results are consistent with the results of comparisons of coincident measurements at 450 nm and 1020 nm between POAM III and SAGE II (C. E. Randall et al., Validation of POAM III version 4.0 aerosols, manuscript in preparation, 2006).

[16] Measurements of balloon-borne OPC and LPC were taken at Syowa Station (69.0°S, 39.6°E, star in Figure 1) by the 43rd and 44th Japanese Antarctic Research Expedition (JARE) on 22 February in 2003 during the ILAS-II preoperational period. Aerosol extinction coefficients estimated from the size distribution measurements were compared to the nearest ILAS-II AEC data. Syowa Station is about 599 km from the nearest ILAS-II measurement location (74.0°S, 36.6°E) on the same day.

[17] Comparisons to data from in situ measurements like OPC and LPC are meaningful even for just one comparison, because the measurement principle differs from that of satellite sensors. A particle counter counts the number of particles and measures their sizes by detecting light scattered by particles that are exposed to incident light. The OPC and LPC use a halogen lamp and a He-Ne laser, respectively, as a light source. The OPC (LPC) measures particles with radii from 0.15 to 3.5 μm (from 0.056 to 0.25 μm). By assuming refractive indices for sulfate aerosols, a bimodal lognormal distribution function was fit to the measured cumulative number concentrations for each particle size range. Extinction at 780 nm was then derived from the particle size distribution by performing Mie scattering calculations. Here, the refractive indices (1.439–1.452) were estimated following *Steele and Hamill* [1981]. Simultaneously observed temperature and pressure data were used, and a mixing ratio of water vapor of 4 ppmv and a sulfate content of an aerosol

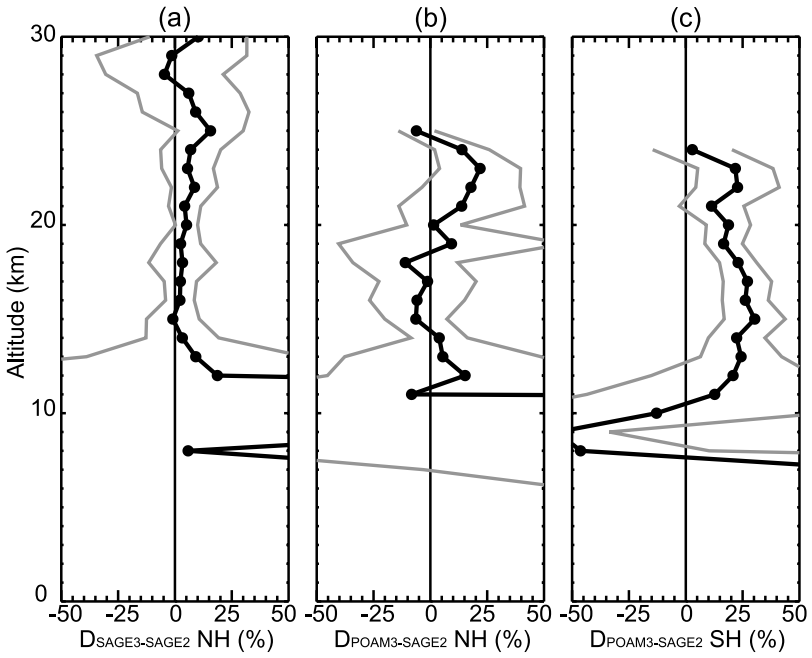

Figure 2. (a) Profiles of the mean difference (black line) between SAGE II (V6.2) and SAGE III (V3.0) aerosol extinction data both interpolated to 780 nm ($\overline{D}_{SAGE3\text{-}SAGE2}$) and the 1σ standard deviation (gray lines) in the NH. Here, the logarithms of SAGE II extinction at 525 nm and 1019 nm and SAGE III extinction at 756 nm and 869 nm are linearly interpolated with the logarithms of the wavelengths, yielding the extinctions at 780 nm. The reported errors of SAGE II and SAGE III extinctions were also interpolated. (b) Profiles of the mean difference between SAGE II and POAM III (V4.0) extinction data at 780 nm ($\overline{D}_{POAM3\text{-}SAGE2}$) and the 1σ standard deviation in the NH. (c) Profiles of the mean difference between SAGE II and POAM III extinction data at 780 nm ($\overline{D}_{POAM3\text{-}SAGE2}$) and the 1σ standard deviation in the SH. Criteria for coincident pairs are a distance from a SAGE II measurement location of no more than 300 km and a measurement time difference of no more than 1 hour for the NH, and a distance of no more than 500 km and a time difference of no more than 12 hours for the SH.

droplet of 1.0×10^{-15} g were assumed. Error in the OPC/LPC data was defined as the RSS of the systematic measurement error and statistical random error of the counting. The systematic measurement error, which includes uncertainty in the flow rate, was around ±5% for all altitude levels. Uncertainty in a count C is $\pm\sqrt{C}$ [e.g., *Willeke and Liu*, 1976]. The relative counting error ($1/\sqrt{C}$) in this study was calculated for each particle size range for each level. The RSS of the calculated counting errors was then defined as the statistical counting error and ranged from 0.4 to 44%.

4. Results

4.1. Northern Hemisphere (NH)

[18] Figure 3 (top) compares ILAS-II extinction to SAGE II extinction in the NH. Here, the relative percent difference, D (%), is defined as follows:

$$D \equiv \frac{100 \times (\text{ILAS-II} - \text{other sensors})}{\frac{1}{2} \times (\text{ILAS-II} + \text{other sensors})}.$$

The RSS of the total error of individual ILAS-II AEC data and the interpolated error of the coincident SAGE II extinction data (defined as "combined error") was divided by the mean of both extinction data, the denominator of the expression for D, to define a relative error. At altitude levels between 12 and 19 km, ILAS-II extinction was within around ±10% of SAGE II extinction; the difference was within the range of the combined error. In contrast, $\overline{D}$ (mean of D) values of ILAS-II and SAGE II from 20 to 26 km ranged from −10 to −34%, which were more than 1σ standard deviation (6–29%). Furthermore, the values exceeded the range of the combined error (7–18%). ILAS-II extinction was smaller than SAGE II extinction when both extinctions were less than $\sim 10^{-4}$ km^{-1}. The mean absolute differences there were as small as $0.7–1.8 \times 10^{-5}$ km^{-1}. One of the possible reasons for the negative bias seen in ILAS-II AEC data is uncertainty in the tangent height registration of the V1.4 retrieval, as described below.

[19] ILAS-II and SAGE III extinction data are compared in Figure 4. As above, D was calculated for each of the ILAS-II and SAGE III coincident pairs. Comparisons between ILAS-II and SAGE III are similar to comparisons between ILAS-II and SAGE II shown in Figure 3 (top). Below 20 km, ILAS-II and SAGE III extinction data were also within around ±10% of each other, and that difference was within the range of the combined error. From 20 to 26 km, ILAS-II extinction values were smaller than SAGE III extinction values; $\overline{D}$ and 1σ standard deviation ranged from -12 ± 8 to -45 ± 26%, exceeding the combined errors (7–21%). However, the difference between ILAS-II and SAGE III occurred when both extinctions were below $\sim 10^{-4}$ km^{-1}, and the magnitude of the mean absolute extinction differences was as small as $1.1–2.2 \times 10^{-5}$ km^{-1}.

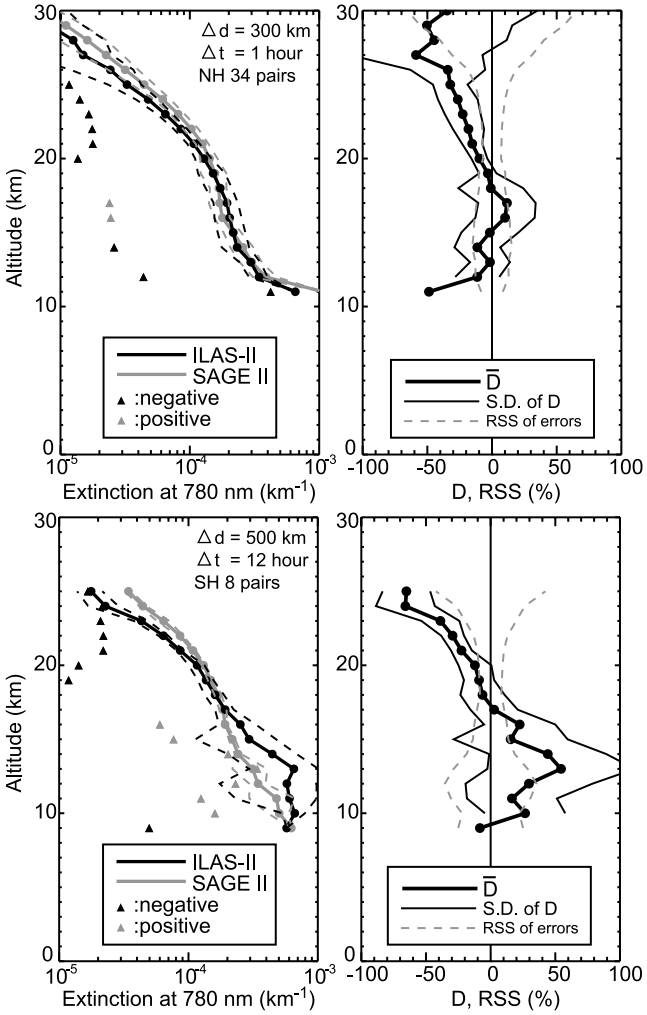

Figure 3. Comparison between ILAS-II and SAGE II extinctions (interpolated to 780 nm) in the NH. (top) 34 coincident pairs in the NH. (bottom) 8 coincident pairs in February in the SH. (left) Profiles of the mean of ILAS-II (black line) and SAGE II (gray line) extinctions used in the comparison. Dashed lines are the 1σ standard deviation profiles. Triangles show the difference between ILAS-II and SAGE II mean extinction values. Black (gray) triangles correspond to negative (positive) values of ILAS-II extinction minus SAGE II extinction. (right) Mean of relative percent difference (D) computed for all coincident ILAS-II and SAGE II extinction data (thick black line) and the 1σ standard deviation (thin black lines). See text for the definition of D. Gray dashed lines indicate the mean of the relative error defined as the RSS of the total error of ILAS-II and the interpolated error of SAGE II divided by the mean of ILAS-II and SAGE II extinctions (equal to the denominator of the expression for D).

[20] Figure 5 (top) compares ILAS-II and POAM III extinction data in the NH. From 11 to 19 km, ILAS-II and POAM III difference was within around ±15% and almost within the range of the combined error. From 20 to 24 km, where both extinctions were less than $\sim 10^{-4}$ km^{-1}, ILAS-II extinction values were small compared to POAM III extinction values. $\overline{D}$ and 1σ standard deviation ranged from −17 ± 12 to −37 ± 25%, exceeding the combined

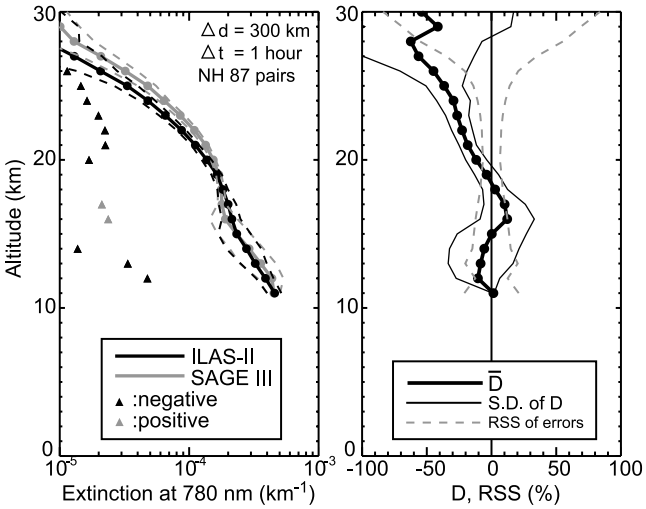

Figure 4. As in Figure 3 but for 87 coincident ILAS-II and SAGE III (interpolated to 780 nm) pairs in the NH.

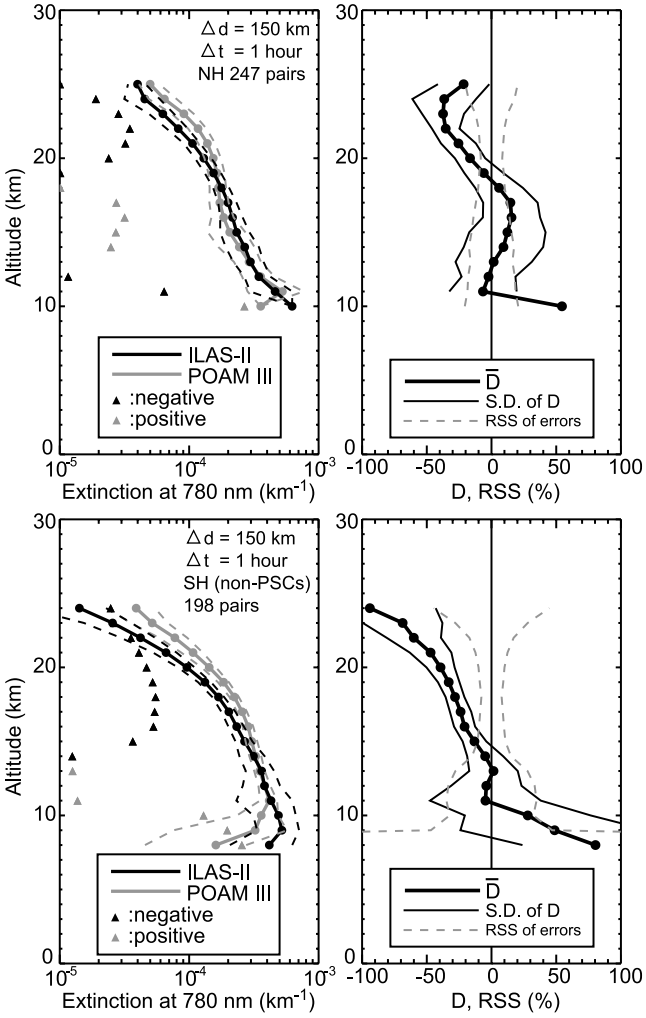

Figure 5. As in Figure 3, but for comparison between ILAS-II and POAM III. (top) 247 coincident pairs in the NH. (bottom) 198 coincident pairs in the non-PSC season in the SH.

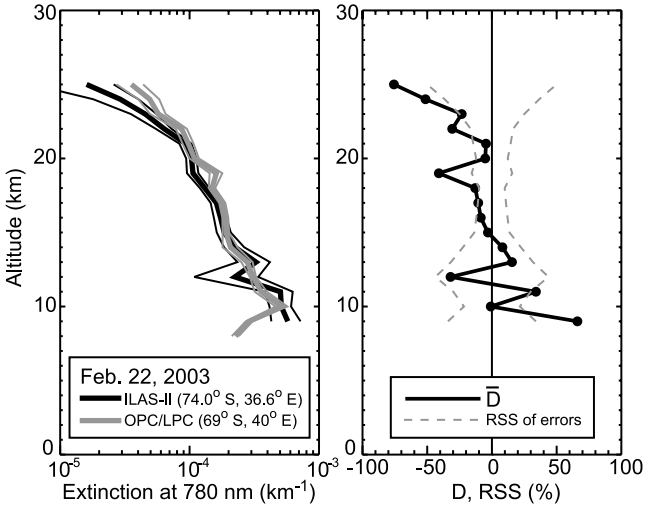

Figure 6. Comparison between ILAS-II (74.0°S, 36.6°E) and OPC/LPC (69.0°S, 39.6°E) on 22 February. The distance between the two measurement locations is 599 km. (left) ILAS-II extinction profile (thick black line) and the total error profile (thin black line). Thick gray and thin gray lines indicate the extinction profile calculated from the OPC/LPC data and the error profile, respectively. See text for the detail of the estimate of error in the OPC/LPC extinction data. (right) Relative percent difference (D) between ILAS-II and OPC/LPC extinction data and the relative error defined as the RSS of the both errors divided by the mean indicated by black and gray dashed lines, respectively.

errors (8–16%). At these altitudes, the magnitudes of the $\overline{D}$ and the mean absolute extinction difference ($1.9–3.5 \times 10^{-5}$ km^{-1}) between ILAS-II and POAM III were slightly larger than those between ILAS-II and SAGE II and those between ILAS-II and SAGE III at the same altitudes.

4.2. Southern Hemisphere (SH)

4.2.1. Non-PSC Season

[21] Figure 3 (bottom) compares ILAS-II and SAGE II extinction data in February. ILAS-II extinction was larger than SAGE II extinction from 10 to 16 km. Four of the eight coincident ILAS-II AEC data were truncated at higher altitudes than usual, around 12–13 km, and the extinction values were unusually large, resulting in poor agreement with SAGE II extinction. However, the other four cases showed good agreement at these altitudes; they agreed to within around ±5% from 12 to 16 km. These two features in the comparison yielded large standard deviations from 10 to 16 km, as shown in Figure 3 (bottom). From 17 to 19 km, ILAS-II and SAGE II were within ±10% of each other. From 20 to 25 km, ILAS-II extinction was smaller than SAGE II extinction. $\overline{D}$ and 1σ standard deviation ranged from −12 ± 12 to −66 ± 23%, exceeding the combined errors (9–24%). These results are similar to those in the NH. ILAS-II extinction was smaller than SAGE II extinction when both extinctions were below $\sim 10^{-4}$ km^{-1}. The mean absolute extinction differences of $1.4–2.2 \times 10^{-5}$ km^{-1} from 20 to 25 km were slightly larger than the absolute differences in the NH ($0.7–1.8 \times 10^{-5}$ km^{-1}).

[22] Figure 5 (bottom) shows comparisons between ILAS-II and POAM III extinctions in the non-PSC season (January–May). They agreed to within ±5% from 11 to 14 km, but ILAS-II extinction was smaller than POAM III extinction above 15 km. $\overline{D}$ and 1σ standard deviation between 15 and 24 km ranged from −13 ± 9 to −94 ± 51%. These values exceeded the combined errors (8–45%). The mean absolute extinction differences of $2.5–5.5 \times 10^{-5}$ km^{-1} were larger than the absolute differences between ILAS-II and SAGE II in the non-PSC season.

[23] Figure 6 shows a comparison between ILAS-II and OPC/LPC data. The differences between the two profiles were comparable to the error bars at most altitude levels. The error in the OPC/LPC data was estimated to be 5–44%; however, this is probably an underestimate, because the systematic error of the measurement and the statistical error of the counting were used as an alternative to the error of the OPC/LPC extinction data. A more proper error estimate would use a Monte Carlo simulation to infer the impact of the measurement uncertainties on the lognormal parameters and the derived parameters such as aerosol extinction, as done by *Deshler et al.* [1993]. The ILAS-II and the OPC/LPC data do agree to within their error bars if the insufficient error estimate is considered. The difference was within ±15% from 13 to 18 km, although ILAS-II extinction was smaller than the OPC/LPC extinction at all levels above 15 km, which is similar to the results in the comparisons with SAGE II and POAM III.

4.2.2. PSC Season

[24] Figure 7 shows comparisons between ILAS-II and POAM III extinction data during the PSC season (June–October). Figure 7 (left) shows that extinction data from both instruments in the PSC season were 5 to 10 times larger than those during the non-PSC season. In addition, both 1σ standard deviations during the PSC season were also larger than those in the non-PSC season, because the height at which PSCs occurred from June to October varied depending on temperature profiles coupled with the movement of cold region. As shown in Figure 7 (right), ILAS-II

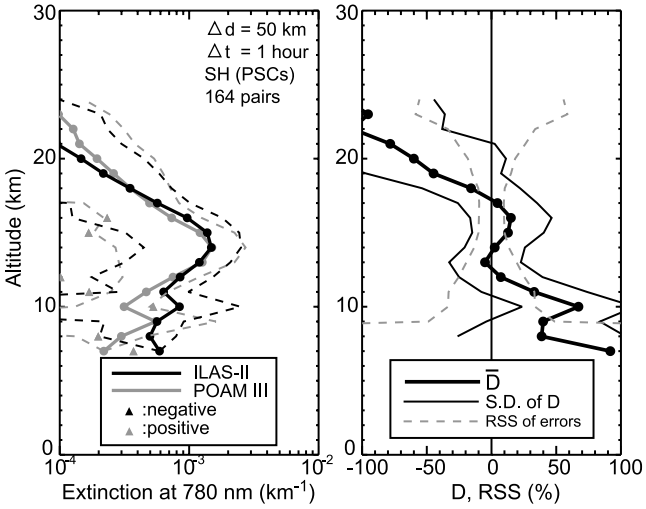

Figure 7. As in Figure 3 but for 164 coincident ILAS-II and POAM III pairs in the PSC season in the SH. Note that the scale of extinction is one order higher than in Figures 3–6.

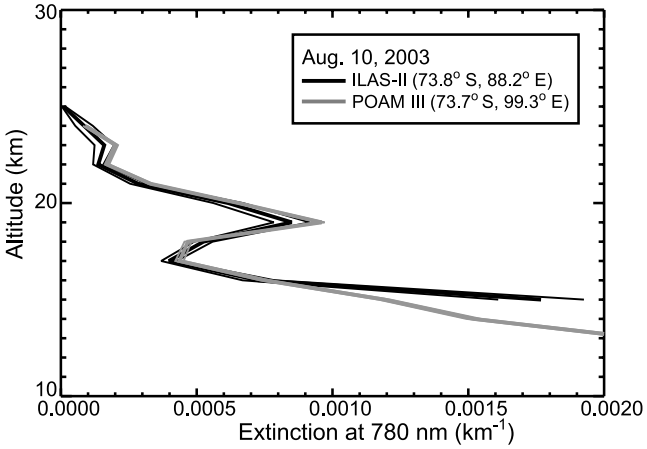

Figure 8. PSC profiles of the ILAS-II (73.8°S, 88.2°E) and the POAM III (73.7°S, 99.3°E) on 10 August 2003 indicated by thick black and gray lines, respectively. Thin lines show their errors. The distance between the two measurement locations and the time difference are 42 km and 0.1 hour.

extinction was smaller than POAM III extinction from 18 to 24 km; $\overline{D}$ ranged from −16 to −112%, exceeding the range of the combined error (10–59%). This characteristic is similar to the results for the non-PSC season in both hemispheres. However, ILAS-II and POAM III extinction data were within ±15% of each other from 12 to 17 km in the PSC season even when PSCs were present.

[25] Figure 8 shows ILAS-II (black) and POAM III (gray) extinction profiles on 10 August 2003. The distance between the two measurement locations and the time difference were no more than 42 km and 0.1 hour. Both profiles included two enhanced layers at approximately 19 km and 23 km, indicating the existence of PSCs. In addition to this case, ILAS-II and POAM III often obtained extinction profiles with vertically layered structures similar to each other when they made observations in very close vicinity.

5. Discussion and Summary

[26] We assessed the data quality of ILAS-II AEC at 780 nm processed with the V1.4 retrieval algorithm. The focus of this study was AEC data below 30 km in the NH and below 25 km in the SH because ILAS-II AEC data above those altitude levels would be affected by sunspots in the current version. Care should therefore be taken when using the V1.4 AEC data above these altitudes. The precision of ILAS-II AEC data as estimated from measurement repeatability was 5–15% at 12–26 km in the NH and 6–20% at 12–23 km in the SH.

[27] In the NH, ILAS-II AEC was ±10% to ±15% of SAGE II, SAGE III, and POAM III below 20 km. Above 20 km, ILAS-II extinction was systematically smaller than extinctions from the other three sensors. The slightly larger differences were seen between ILAS-II and SAGE III/POAM III extinction data than between ILAS-II and SAGE II extinction data, because SAGE III and POAM III extinction values were slightly larger on average than SAGE II extinction values (Figures 2a and 2b). It is also consistent with the generally larger variability in POAM III extinction data than in SAGE II extinction data at 1020 nm [*Randall et al.*, 2001, Figure 6].

[28] ILAS-II and SAGE II comparisons for February in the SH suggest that ILAS-II AEC has a negative bias ranging from −12 to −66% as altitude increases from 20 to 25 km, although their agreement was closer from 17 to 19 km. The magnitude of $\overline{D}$ between ILAS-II and SAGE II over the SH was slightly larger than that over the NH at the same altitude levels. It is still unclear why differences were larger in the SH than in the NH above 20 km. ILAS-II extinction was systematically smaller than POAM III extinction at all levels above 15 km during the non-PSC season (January–May). The difference was larger than the difference between ILAS-II and SAGE II. However, in contrast to the NH, POAM III extinction data have a distinct positive bias relative to SAGE II extinction data in the SH (Figure 2c). The bias can explain why ILAS-II AEC data have a larger negative bias against POAM III data during the non-PSC season in the SH. During the PSC season (June–October), ILAS-II extinction agreed with POAM III extinction from 12 to 17 km despite the high frequency of PSC, although ILAS-II was also smaller than POAM III above 18 km.

[29] Uncertainty in tangent height registration is one possible cause for extinction differences between ILAS-II and three other satellite sensors above approximately 20 km. Tangent height registration error can induce error in retrieved extinction data. Uncertainties in tangent height registration were less than 100 m for the SAGE II V6.2 retrieval, around 100 m for the SAGE III V3.0 retrieval [*Wang et al.*, 2002; J. Zawodny, personal communication, 2005], and 250 m for the POAM III V4.0 retrieval [*Lumpe et al.*, 2002; J. Lumpe, personal communication, 2005]. In the ILAS-II V1.4 retrieval, the transmittance spectrum method (TS-M) is applied to determine tangent heights below 30 km. The TS-M utilizes the fact that the absorption spectra due to oxygen molecules (O_2 A-band) are expressed as a function of temperature and pressure profiles [*Nakajima et al.*, 2002]. Uncertainty in the TS-M mainly arises from error in estimating the baseline component, consisting of aerosol scattering, Rayleigh scattering by atmospheric molecules, and absorption by ozone in the Wulf band (referred to as the "baseline fitting error"), and error in selecting the range of the O_2 A-band for calculating the transmittance spectra ("range selection error"). Numerical simulations that were similar to those applied by *Nakajima et al.* [2002] showed that errors in the baseline fitting and range selection would systematically shift the registered tangent heights, producing systematic errors ranging from −100 to +100 m and from −150 to +150 m, respectively. Including uncertainties in ILAS-II geometric position and instrument functions, the uncertainty in the tangent height registration below 30 km for the ILAS-II V1.4 retrieval is systematic error ranging from −180 to 180 m and random error of ±30 m (T. Tanaka et al., New tangent height registration method with version 1.4 data retrieval algorithm for the solar occultation sensor ILAS-II, manuscript in preparation, 2006).

[30] A sensitivity study using ILAS-II data suggested that height assignments 100 m higher than in the current retrieval caused a ~5% increase in AEC below 20 km

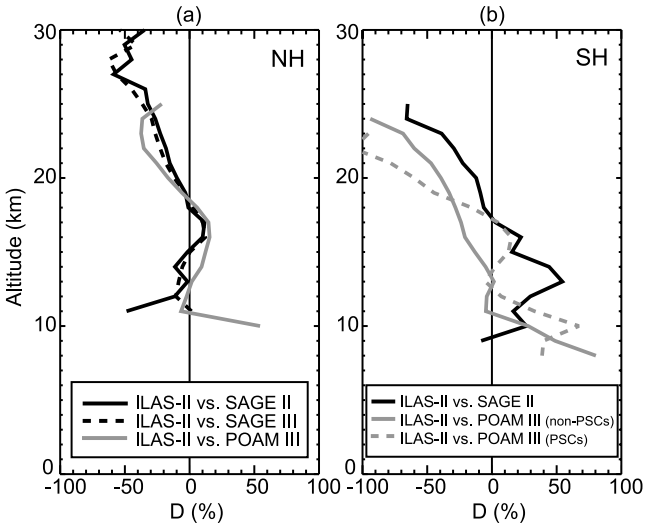

Figure 9. Mean profiles of relative percent difference (D) between ILAS-II and SAGE II, SAGE III, or POAM III. They are identical with the values shown in the right plots of Figures 3, 4, 5, and 7. (a) NH. (b) SH.

and a 10–25% increase at approximately 25 km; reversely, height assignments 100 m lower than in the current retrieval caused ~5% and 10–25% decreases in AEC below 20 km and at approximately 25 km, respectively. If a height assignment becomes 100 m higher than the current retrieval, the negative bias seen in ILAS-II AEC data above approximately 20 km in both hemispheres disappears for the most part. The higher altitude assignment also increases AEC below approximately 20 km where ILAS-II extinction was slightly larger than extinctions from the other sensors although the difference was within retrieval errors. However, it does not produce any noticeable bias at lower altitude levels because the percentage of the impact of uncertainty in the tangent height registration on retrieved AEC decreased with decreasing altitudes.

[31] Figure 9 summarizes the comparisons of aerosol extinction data between ILAS-II and other satellite sensors in both hemispheres. Over the NH, the magnitudes of relative differences in extinctions between ILAS-II and three other sensors were similar, and the difference characteristics in the vertical were also similar. Over the SH, the magnitudes of relative differences between ILAS-II extinction and SAGE II and POAM III extinctions were different. Above approximately 20 km in both hemispheres, ILAS-II AEC is systematically lower, but the mean absolute difference is as small as $\sim 2 \times 10^{-5}$ km^{-1} during the non-PSC season.

[32] **Acknowledgments.** We thank all members of the ILAS-II Science Team and Validation Experiment Team and their associates. We are also grateful to the United Kingdom Meteorological Office (Met Office) for supplying the Met Office assimilation data. OPC/LPC measurements at Syowa Station for ILAS-II validation were carried out by the 43rd and 44th Japanese Antarctic Research Expedition (JARE) in cooperation with the National Institute of Polar Research (NIPR) and the ILAS-II project of the National Institute for Environmental Studies (NIES) with help of Japan Meteorological Agency (JMA). The ILAS-II data retrieval processing was carried out at the ILAS-II Data Handling Facility (DHF) at NIES. The ILAS-II project has been funded by the Ministry of the Environment of Japan (MOE). A part of this research work was supported with the Global Environment Research Fund provided by MOE.

References

Ackerman, M., et al. (1989), European validation of SAGE II aerosol profiles, *J. Geophys. Res.*, *94*, 8399–8411.

Bevilacqua, R. M., et al. (2002), Observations and analysis of polar stratospheric clouds detected by POAM III during the 1999/2000 Northern Hemisphere winter, *J. Geophys. Res.*, *107*(D20), 8281, doi:10.1029/2001JD000477.

Burton, S. P., L. W. Thomason, Y. Sasano, and S. Hayashida (1999), Comparison of aerosol extinction measurements by ILAS and SAGE II, *Geophys. Res. Lett.*, *26*, 1719–1722.

Deshler, T., B. J. Johnson, and W. R. Rozier (1993), Balloonborne measurements of Pinatubo aerosol during 1991 and 1992 at 41 N: Vertical profiles, size distribution, and volatility, *Geophys. Res. Lett.*, *20*, 1435–1438.

Fromm, M. D., J. D. Lumpe, R. M. Bevilacqua, E. P. Shettle, J. Hornstein, S. T. Massie, and K. H. Fricke (1997), Observations of Antarctic polar stratospheric clouds by POAM II: 1994–1996, *J. Geophys. Res.*, *102*, 23,659–23,672.

Fromm, M. D., R. M. Bevilacqua, J. Hornstein, E. Shettle, K. Hoppel, and J. D. Lumpe (1999), An analysis of Polar Ozone and Aerosol Measurement (POAM) II Arctic polar stratospheric cloud observations, 1993–1996, *J. Geophys. Res.*, *104*, 24,341–24,357.

Hayashida, S., N. Saitoh, A. Kagawa, T. Yokota, M. Suzuki, H. Nakajima, and Y. Sasano (2000), Arctic polar stratospheric clouds observed with the Improved Limb Atmospheric Spectrometer during winter 1996/1997, *J. Geophys. Res.*, *105*, 24,715–24,730.

Hervig, M., and T. Deshler (2002), Evaluation of aerosol measurements from SAGE II, HALOE, and balloonborne optical particle counters, *J. Geophys. Res.*, *107*(D3), 4031, doi:10.1029/2001JD000703.

Hitchman, M., M. McKay, and C. Trepte (1994), A climatology of stratospheric aerosol, *J. Geophys. Res.*, *99*, 20,689–20,700.

International Organization for Standardization (1993), Guide to the expression of uncertainty in measurement, 100 pp., Tech. Advis. Group on Meteorol., Geneva, Switzerland.

Lumpe, J. D., R. M. Bevilacqua, K. W. Hoppel, and C. E. Randall (2002), POAM III retrieval algorithm and error analysis, *J. Geophys. Res.*, *107*(D21), 4575, doi:10.1029/2002JD002137.

McCormick, M. P., H. M. Steele, P. Hamill, W. P. Chu, and T. J. Swissler (1982), Polar stratospheric cloud sightings by SAM II, *J. Atmos. Sci.*, *39*, 1387–1397.

Nakajima, H., et al. (2002), Tangent height registration for the solar occultation satellite sensor ILAS: A new technique for version 5.20 products, *J. Geophys. Res.*, *107*(D24), 8215, doi:10.1029/2001JD000607.

Nakajima, H., T. Sugita, T. Yokota, and Y. Sasano (2004), Current status and early result of the ILAS-II onboard the ADEOS-II satellite, in *Sensors, Systems, and Next Generation Satellites IX*, *Proc. SPIE Int. Soc. Opt. Eng.*, *5234*, 36–46.

Nakajima, H., et al. (2006), Characteristics and performance of the Improved Limb Atmospheric Spectrometer-II (ILAS-II) on board the ADEOS-II satellite, *J. Geophys. Res.*, doi:10.1029/2005JD006334, in press.

Nash, E. R., P. A. Newman, J. E. Rosenfield, and M. R. Schoeberl (1996), An objective determination of the polar vortex using Ertel' s potential vorticity, *J. Geophys. Res.*, *101*, 9471–9478.

Osborn, M. T., J. M. Rosen, M. P. McCormick, P.-H. Wang, J. M. Livingston, and T. J. Swissler (1989), SAGE II aerosol correlative observations: Profile measurements, *J. Geophys. Res.*, *94*, 8353–8366.

Poole, L. R., and M. C. Pitts (1994), Polar stratospheric cloud climatology based on Stratospheric Aerosol Measurement II observations from 1978 to 1989, *J. Geophys. Res.*, *99*, 13,083–13,089.

Poole, L. R., C. R. Trepte, V. L. Harvey, G. C. Toon, and R. L. VanValkenburg (2003), SAGE III observations of Arctic polar stratospheric clouds – December 2002, *Geophys. Res. Lett.*, *30*(23), 2216, doi:10.1029/2003GL018496.

Randall, C. E., D. W. Rusch, J. J. Olivero, R. M. Bevilacqua, L. R. Poole, J. D. Lumpe, M. D. Fromm, K. W. Hoppel, J. S. Hornstein, and E. P. Shettle (1996), An overview of POAM II aerosol measurements at 1.06 μm, *Geophys. Res. Lett.*, *23*, 3195–3198.

Randall, C. E., R. M. Bevilacqua, J. D. Lumpe, K. W. Hoppel, D. W. Rusch, and E. P. Shettle (2000), Comparison of Polar Ozone and Aerosol Measurement (POAM) II and Stratospheric Aerosol and Gas Experiment (SAGE) II aerosol measurements from 1994 to 1996, *J. Geophys. Res.*, *105*, 3929–3942.

Randall, C. E., R. M. Bevilacqua, J. D. Lumpe, and K. W. Hoppel (2001), Validation of POAM III aerosol: Comparison to SAGE II and HALOE, *J. Geophys. Res.*, *106*, 27,525–27,536.

Russell, P. B., and M. P. McCormick (1989), SAGE II aerosol data validation and initial data use: An introduction and overview, *J. Geophys. Res.*, *94*, 8335–8338.

Saitoh, N., S. Hayashida, Y. Sasano, and L. L. Pan (2002), Characteristics of Arctic polar stratospheric clouds in the winter of 1996/1997 inferred from ILAS measurements, *J. Geophys. Res.*, *107*(D24), 8205, doi:10.1029/2001JD000595.

Sasano, Y., M. Suzuki, T. Yokota, and H. Kanzawa (1995), Improved Limb Atmospheric Spectrometer (ILAS) project: ILAS instrument, performance and validation plan, *Proc. SPIE Int. Soc. Opt. Eng.*, *2583*, 193–204.

Sasano, Y., M. Suzuki, T. Yokota, and H. Kanzawa (1999), Improved Limb Atmospheric Spectrometer (ILAS) for stratospheric ozone layer measurements by solar occultation technique, *Geophys. Res. Lett.*, *26*, 197–200.

Sasano, Y., T. Yokota, H. Nakajima, T. Sugita, and H. Kanzawa (2001), ILAS-II instrument and data processing system for stratospheric ozone layer monitoring, *Proc. SPIE Int. Soc. Opt. Eng.*, *4150*, 106–114.

Solomon, S. (1999), Stratospheric ozone depletion: A review of concepts and history, *Rev. Geophys.*, *37*, 275–316.

Steele, H. M., and P. Hamill (1981), Effects of temperature and humidity on the growth and optical properties of sulphuric acid-water droplets in the stratosphere, *J. Aerosol Sci.*, *12*, 517–528.

Stratospheric Processes and their Role in Climate (2005), SPARC assessment of stratospheric aerosol properties, edited by L. W. Thomason and T. Peter, *WCRP-124, WMO/TD 1295, SPARC Rep. 4*, World Clim. Res. Programme, Geneva, Switzerland.

Strawa, A. W., K. Drdla, M. Fromm, R. F. Pueschel, K. W. Hoppel, E. V. Browell, P. Hamill, and D. P. Dempsey (2002), Discriminating Types Ia and Ib polar stratospheric clouds in POAM satellite data, *J. Geophys. Res.*, *107*(D20), 8291, doi:10.1029/2001JD000458.

Taha, G., L. W. Thomason, C. R. Trepte, and W. P. Chu (2004), Validation of SAGE III data products version 3.0, paper presented at Quadrennial Ozone Symposium, Int. Ozone, Comm., Int. Assoc. for Meteorol. and Atmos. Sci., Kos, Greece.

Thomason, L. W. (1991), A diagnostic stratospheric aerosol size distribution inferred from SAGE II measurements, *J. Geophys. Res.*, *96*, 22,501–22,508.

Thomason, L. W., and L. R. Poole (1993), Use of stratospheric aerosol properties as diagnostics of Antarctic vortex processes, *J. Geophys. Res.*, *98*, 23,003–23,012.

Thomason, L. W., and G. Taha (2003), SAGE III aerosol extinction measurements: Initial results, *Geophys. Res. Lett.*, *30*(12), 1631, doi:10.1029/2003GL017317.

Thomason, L. W., L. R. Poole, and T. Deshler (1997), A global climatology of stratospheric aerosol surface area density deduced from Stratospheric Aerosol and Gas Experiment II measurements: 1984–1994, *J. Geophys. Res.*, *102*, 8967–8976.

Wang, H. J., D. M. Cunnold, L. W. Thomason, J. M. Zawodny, and G. E. Bodeker (2002), Assessment of SAGE version 6.1 ozone data quality, *J. Geophys. Res.*, *107*(D23), 4691, doi:10.1029/2002JD002418.

Willeke, K., and B. Liu (1976), Single particle optical counter: Principle and application, in *Fine Particles*, edited by B. Y. H. Liu, pp. 697–729, Elsevier, New York.

World Meteorological Organization (2002), Scientific assessment of ozone depletion, Geneva, Switzerland.

Yokota, T., H. Nakajima, T. Sugita, H. Tsubaki, Y. Itou, M. Kaji, M. Suzuki, H. Kanzawa, J. H. Park, and Y. Sasano (2002), Improved Limb Atmospheric Spectrometer (ILAS) data retrieval algorithm for Version 5.20 gas profile products, *J. Geophys. Res.*, *107*(D24), 8216, doi:10.1029/2001JD000628.

R. M. Bevilacqua, Naval Research Laboratory, Code 413BE, Remote Sensing Division, 4555 Overlook Avenue, Washington, DC 20375, USA.

M. K. Ejiri, Center for Atmospheric and Space Sciences, Utah State University, Logan, UT 84322, USA.

M. Hayashi and K. Shiraishi, Faculty of Science, Fukuoka University, Fukuoka 814-0180, Japan.

S. Hayashida, Faculty of Science, Nara Women's University, Nara 630-8506, Japan.

H. Irie, Frontier Research Center for Global Change, Japan Agency for Marine-Earth Science and Technology, Yokohama 236-0001, Japan.

H. Kanzawa, Department of Earth and Environmental Science, Graduate School of Environmental Studies, Nagoya University, Nagoya 464-8601, Japan.

H. Kobayashi, Central Research Institute of Electric Power Industry, 2-11-1 Iwadokita, Komae-shi, Tokyo 201-8511, Japan.

H. Nakajima, Y. Sasano, T. Sugita, T. Tanaka, and T. Yokota, National Institute for Environmental Studies, Tsukuba 305-0053, Japan.

C. E. Randall, Laboratory for Atmospheric and Space Physics, University of Colorado, Boulder, CO 80303, USA.

N. Saitoh, Center for Climate System Research, University of Tokyo, General Research Building, 5-1-5 Kashiwanoha, Kashiwa-shi, Chiba 277-8568, Japan. (snaoko@ccsr.u-tokyo.ac.jp)

G. Taha, Science Systems and Applications, Inc., 10210 Greenbelt Road, Suite 400, Lanham, MD 20706, USA.

Y. Terao, Division of Engineering and Applied Science and Technology, Harvard University, Cambridge, MA 02138, USA.

L. W. Thomason, NASA Langley Research Center, 23a Langley Boulevard, MS 475, Hampton, VA 23681, USA.